Supplementary file

In-situ observation and mechanistic investigation of bubble-size effects on gas hydrate formation and dissociation at the pore scale

Leyan Wen[1], Changqi Li[1], Ruilu Zhang[1], Yang Yu[1,2], Yajun Deng[1,*], Hailong Lu[3]

[1] *Future Technology School, Shenzhen Technology University, Shenzhen 518118, P. R. China*

[2] *School of Safety Science, Tsinghua University, Beijing 100084, P. R. China*

[3] *Beijing International Center for Gas Hydrate, School of Earth and Space Sciences, Peking University, Beijing 100871, P. R. China*

E-mail address: heyoukeke@gmail.com (L. Wen); lcq13428528568@163.com (C. Li); amnesiatoma@outlook.com (R. Zhang); yuyang1@mail.tsinghua.edu.cn (Y. Yu); dengyajun@sztu.edu.cn (Y. Deng); hlu@pku.edu.cn (H. Lu).

*Corresponding author (ORCID: 0000-0003-0554-1466 (Y. Deng))

Wen, L., Li, C., Zhang, R., Yu, Y., Deng, Y., Lu, H. In-situ observation and mechanistic investigation of bubble-size effects on gas hydrate formation and dissociation at the pore scale. Advances in Geo-Energy Research, 2026, 21(3): 283-296.

The link to this file is: https://doi.org/10.46690/ager.2026.09.07

Appendix A: Supplementary figures

The following supplementary figures provide additional pore-scale observations supporting the two-stage hydrate formation and dissociation mechanisms described in the main text.

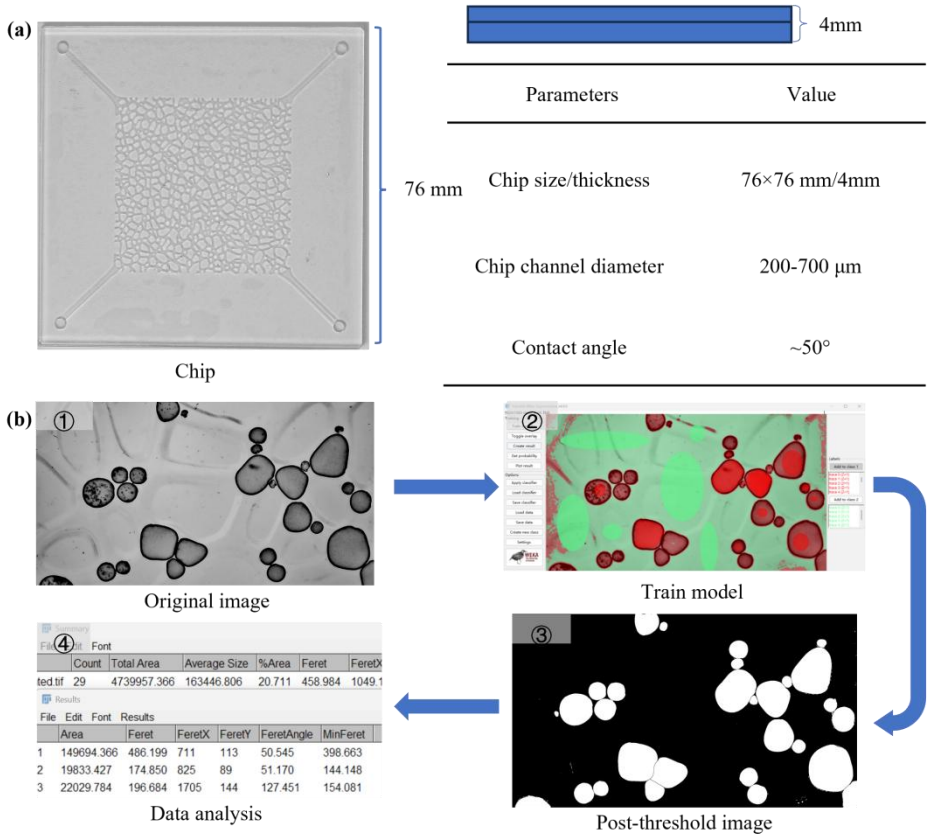


Fig. S1. Microfluidic chip and image-analysis workflow. (a) Chip morphology and dimensions; (b) procedure for obtaining quantitative measurements.

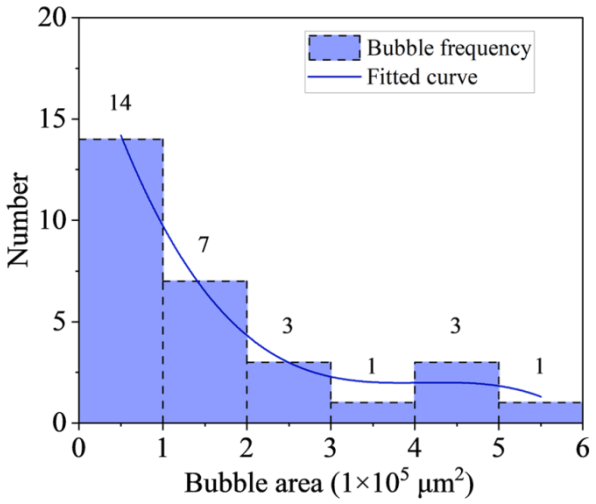


Fig. S2. Size distribution of the initial gas bubbles. The histogram shows projected bubble area, with the fitted curve in blue.

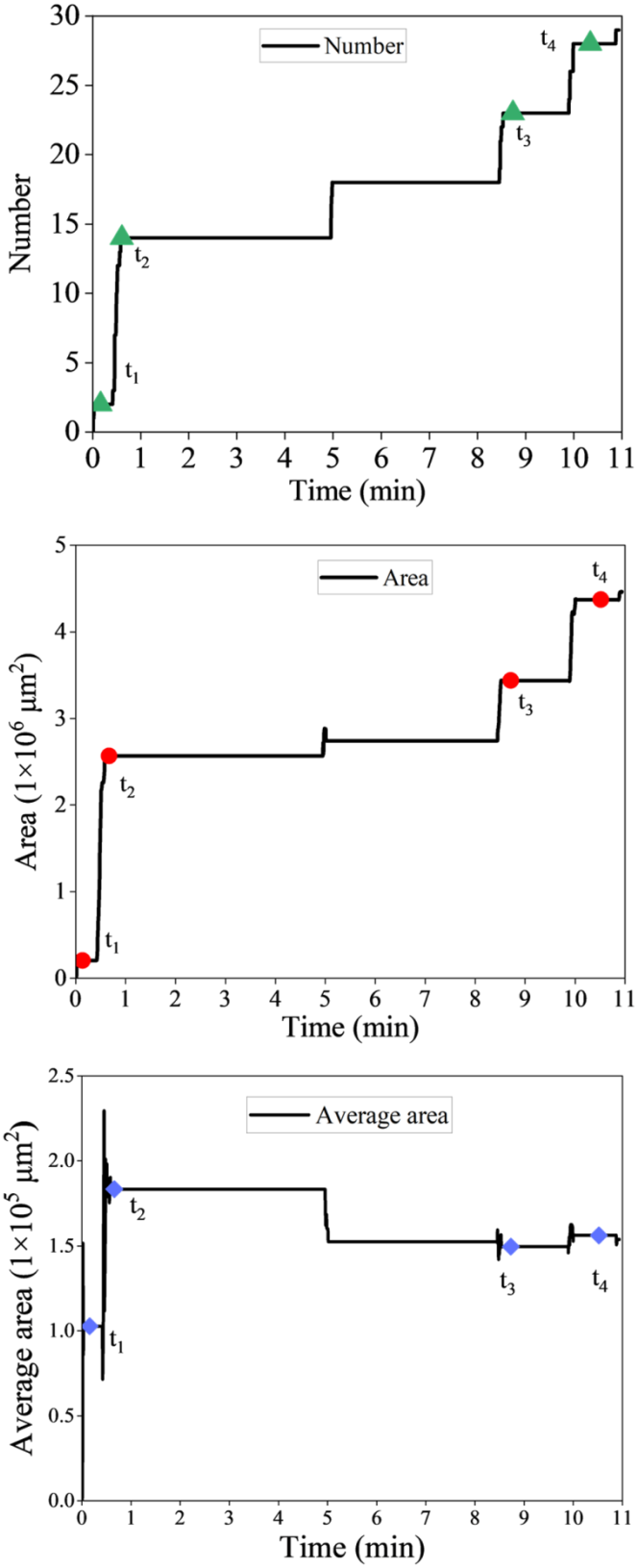


Fig. S3. Temporal changes in porous hydrate shells. Shell number, total projected area, and average projected area against time.

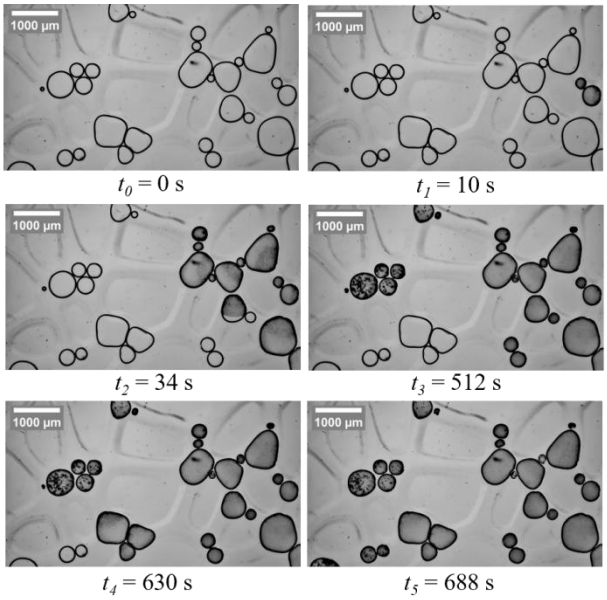


Fig. S4. Hydrate shell growth at pore throats. Selected micrographs show shells forming and connecting between neighboring bubbles.

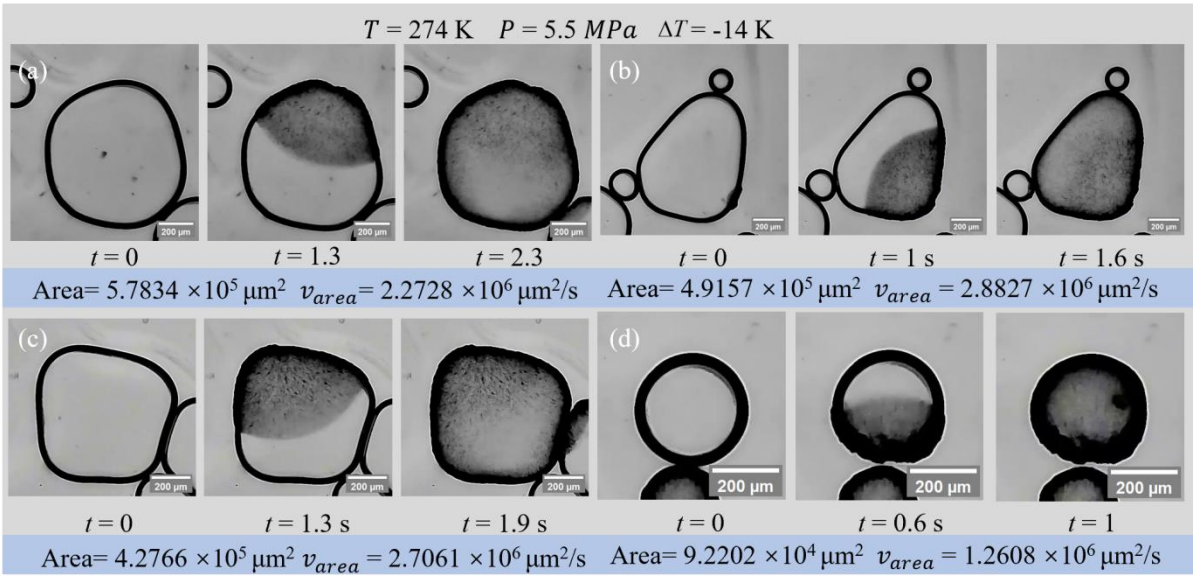


Fig. S5. Hydrate film propagation on bubbles of different sizes at 274 K and 5.5 MPa. (a-d) Representative time-lapse sequences.

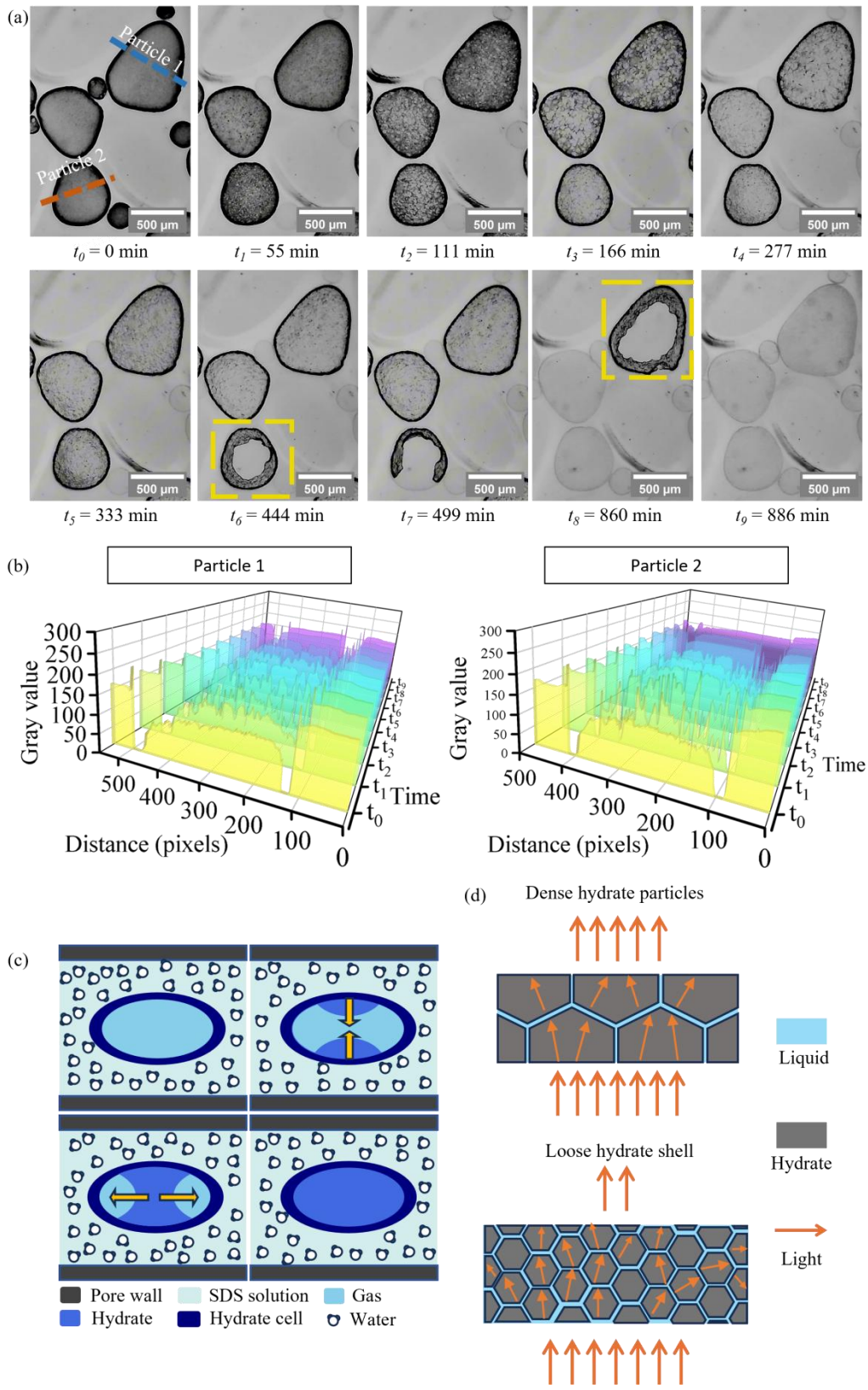


Fig. S6. Morphological and optical changes during hydrate densification. (a) Time-lapse images; (b) gray-scale profiles; (c) inward densification schematic; (d) optical transmission comparison.

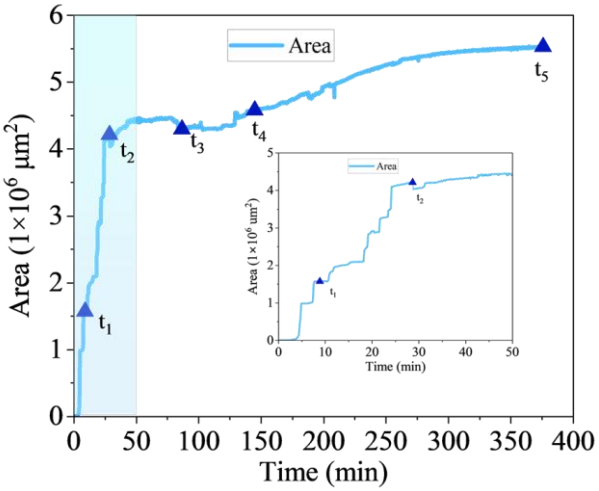


Fig. S7. Projected bubble area during hydrate dissociation. The inset shows the rapid initial stage.

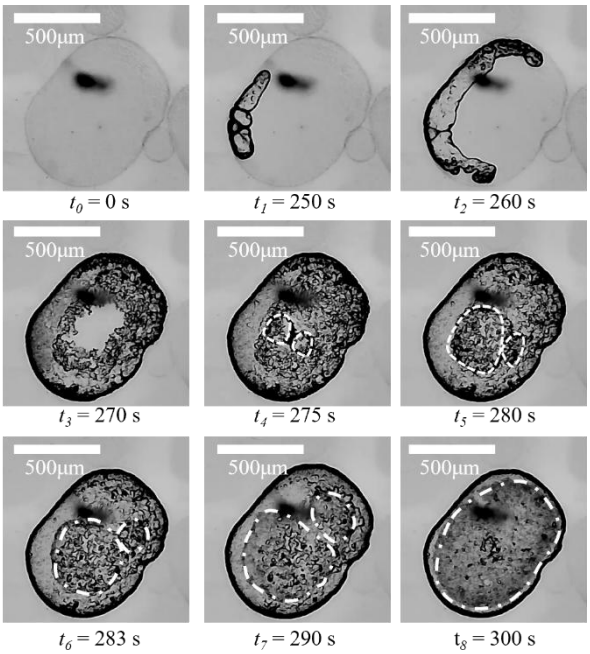


Fig. S8. Stage I internal dissociation of a dense hydrate grain. White dashed lines mark internal microbubbles.

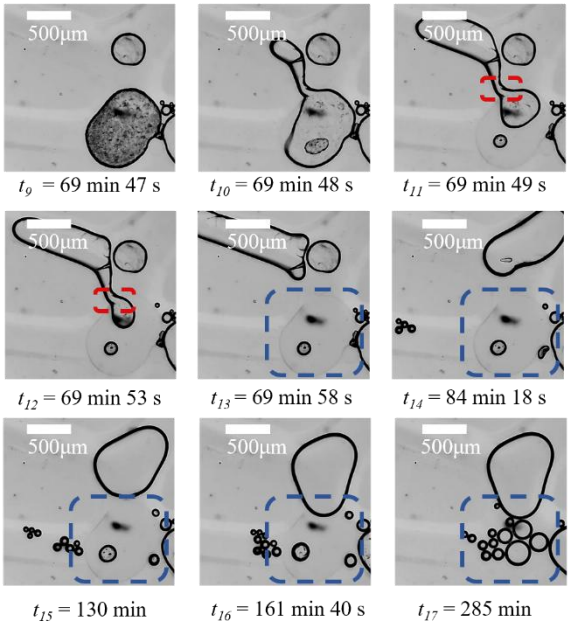


Fig. S9. Stage II outer hydrate shell dissociation. Red dashed lines mark breaches; blue boxes indicate remaining shell fragments.

Appendix B: Supplementary nomenclature and equation index

The following equations and nomenclature provide the kinetic and diffusive transport model definitions referenced in the main text. Table S1 lists the equations and their descriptions. Table S2 defines the symbols, units, and corresponding equation numbers for this model. Geometric descriptors used outside this model, including the projected area A_proj and the mathematical constant π, are defined in the main text. In the equations, d denotes the upright differential operator; vectors are set in bold, whereas scalars are not bold.

Table S1. Equations and descriptions of the kinetic and diffusive transport models used in this study.

Eq.	Expression	Description / Note
1	$G + n_h\mathrm{H_2O} \leftrightarrow G \cdot n_h\mathrm{H_2O}$	Elementary reaction at the hydrate growth front
2	$r_h = k'(c^* - c_e)$	Molar formation rate of the hydrate shell
3	$k' = k_r(\frac{\rho_w}{M_w})^{n_h}$	Apparent rate constant defined from the intrinsic rate constant
4	$r_h = \frac{\rho_h}{M_h} v_f$	Molar balance at the growth front
5	$v_f = \frac{M_h k'(c^* - c_e)}{\rho_h}$	Growth-front velocity
6	$\boldsymbol{J} = \beta(c_s - c^*) = \lvert r_g \rvert$	Molar flux of dissolved gas equals gas consumption rate
7	$r_h = -r_g$	Relation between hydrate formation and gas consumption

8	$c^* = \frac{k'c_e + \beta c_s}{k' + \beta}$	Gas concentration at the growth front
9	$v_f = \frac{M_h k^* \Delta c}{\rho_h}$	Growth-front velocity with combined rate constant
10	$\frac{1}{k^*} = \frac{1}{k'} + \frac{1}{\beta}$	Overall (combined) rate constant
11	$v_a = v_f C_p$	Areal growth rate from front velocity and perimeter
12	$C_p \propto R_e$	Perimeter scaling with equivalent circular radius
13	$\frac{\mathrm{d}n_p}{\mathrm{d}t} = {K_1}^* A_p (f - f_e)$	Molar hydrate formation rate for a single hydrate particle (Englezos et al., 1987).
14	$\frac{1}{{K_1}^*} = \frac{1}{k_r} + \frac{1}{k_d}$	Overall kinetic rate constant combining interfacial reaction and shell mass-transfer resistances.
15	$k_r = k_0 \exp\left(-\frac{\Delta E_a}{RT}\right)$	Arrhenius temperature dependence of the hydrate formation rate constant (Laidler, 1984).
16	$V_p = C_1 {R_e}^3, A_p = C_2 {R_e}^2$	Geometric relationships between particle volume, surface area, and equivalent radius.
17	$\frac{\mathrm{d}n_p}{\mathrm{d}t} t_d = \frac{V_p \rho_h}{M_h}$	Molar balance between hydrate formation and the accumulated hydrate mass.
18	$t_d = \frac{C_1 {R_e}^3 \rho_h}{{K_1}^* C_2 {R_e}^2 (f - f_e) M_h}$	Total densification time derived from Eqs. (13), (16), and (17).
19	$t_d = \frac{1}{3} \frac{\rho_h R_e}{{K_1}^* (f - f_e) M_h}$	Final total densification time for an ideal spherical hydrate particle.
20	$\boldsymbol{J} = -D_e \frac{\mathrm{d}c}{\mathrm{d}x}$	Fick's first law for diffusion-limited gas transport through the hydrate shell (Fick, 1855).

Table S2. Symbols, definitions, units, and corresponding equations for the kinetic and diffusive transport models.

Symbol	Definition	Unit / Dimension	Eq.
G	Guest gas molecule (e.g., CH_4)	—	1
$\mathrm{H_2O}$	Water molecule	—	1
$\mathrm{G} \cdot n_\mathrm{h} \mathrm{H_2O}$	Hydrate formula unit	—	1
n_h	Hydration number	— (dimensionless)	1, 3
r_h	Molar formation rate of hydrate shell	$\mathrm{mol/m^2 s}$	2, 4, 7
k'	Apparent interfacial rate constant	$\mathrm{m/s}$	2, 3, 5, 8, 10
c^*	Molar concentration of dissolved gas at the growth front	$\mathrm{mol/m^3}$	2, 5, 6, 8
c_e	Gas concentration at liquid–solid–gas three-phase equilibrium	$\mathrm{mol/m^3}$	2, 5, 8
k_i	Intrinsic interfacial rate constant	$\mathrm{m/s(m^3/mol)^{n_h}}$	3

ρ_w	Mass density of the aqueous phase	$\mathrm{kg/m^3}$	3
M_w	Molar mass of water	$\mathrm{kg/mol}$	3
ρ_h	Mass density of the hydrate	$\mathrm{kg/m^3}$	4, 5, 9, 17, 18, 19
M_h	Molar mass of the hydrate	$\mathrm{kg/mol}$	4, 5, 9, 17, 18, 19
v_f	Growth-front velocity along the three-phase boundary	$\mathrm{m/s}$	4, 5, 9, 11
c_s	Dissolved-gas concentration at the gas–liquid interface	$\mathrm{mol/m^3}$	6, 8
β	Mass-transfer coefficient of dissolved gas	$\mathrm{m/s}$	6, 8, 10
r_g	Molar rate of gas consumption	$\mathrm{mol/m^2s}$	6, 7
$\boldsymbol{J}$	Molar flux vector of gas at the growth front and through the hydrate shell	$\mathrm{mol/m^2s}$	6, 20
Δc	Concentration driving force (molar concentration difference)	$\mathrm{mol/m^3}$	9
k^*	Overall (combined) rate constant of growth front	$\mathrm{m/s}$	9, 10
v_a	Areal growth rate of the hydrate film	$\mathrm{m^2/s}$	11
C_p	Perimeter of the growth front (three-phase line)	m	11, 12
R_e	Equivalent circular radius derived from the projected area of the bubble or particle (2D descriptor)	m	12, 16, 18, 19
$\frac{\mathrm{dn}_p}{\mathrm{d}t}$	Molar hydrate formation rate per particle	$\mathrm{mol/s}$	13, 17
${K_1}^*$	Overall kinetic rate constant combining interfacial reaction and shell mass transfer	$\mathrm{mol/m^2sPa}$	13, 14, 18, 19
A_p	Outer surface area of the hydrate particle	$\mathrm{m^2}$	13, 16
n_p	Moles of hydrate formed in an individual particle	mol	13, 17
t	Time	s	13, 17
f	Fugacity of dissolved gas	Pa	13, 18, 19
f_e	Equilibrium fugacity	Pa	13, 18, 19
k_r	Interfacial reaction rate constant; temperature dependence given by Eq. (15)	$\mathrm{mol/m^2sPa}$	14, 15
k_d	Cross-shell mass-transfer rate constant	$\mathrm{mol/m^2sPa}$	14
k_0	Pre-exponential factor in the Arrhenius relationship	$\mathrm{mol/m^2sPa}$	15
ΔE_a	Activation energy	J/mol	15
R	Universal gas constant	J/molK	15
T	Local temperature	K	15

V_{p}	Volume of an individual hydrate particle	m^3	16, 17
C_1	Geometric shape factor for particle volume	dimensionless	16, 18
C_2	Geometric shape factor for particle surface area	dimensionless	16, 18
t_d	Total densification time	s	17, 18, 19
D_e	Effective diffusion coefficient of gas in the hydrate shell	m^2/s	20
c	Dissolved-gas concentration	$\mathrm{mol}/\mathrm{m}^3$	20
x	Diffusion path coordinate	m	20
$\frac{\mathrm{d}c}{\mathrm{d}x}$	Concentration gradient along the diffusion direction	$\mathrm{mol}/\mathrm{m}^4$	20